Photocathodes and the LCSL-II Injector

Theodore Vecchione

LCLS-II Overview

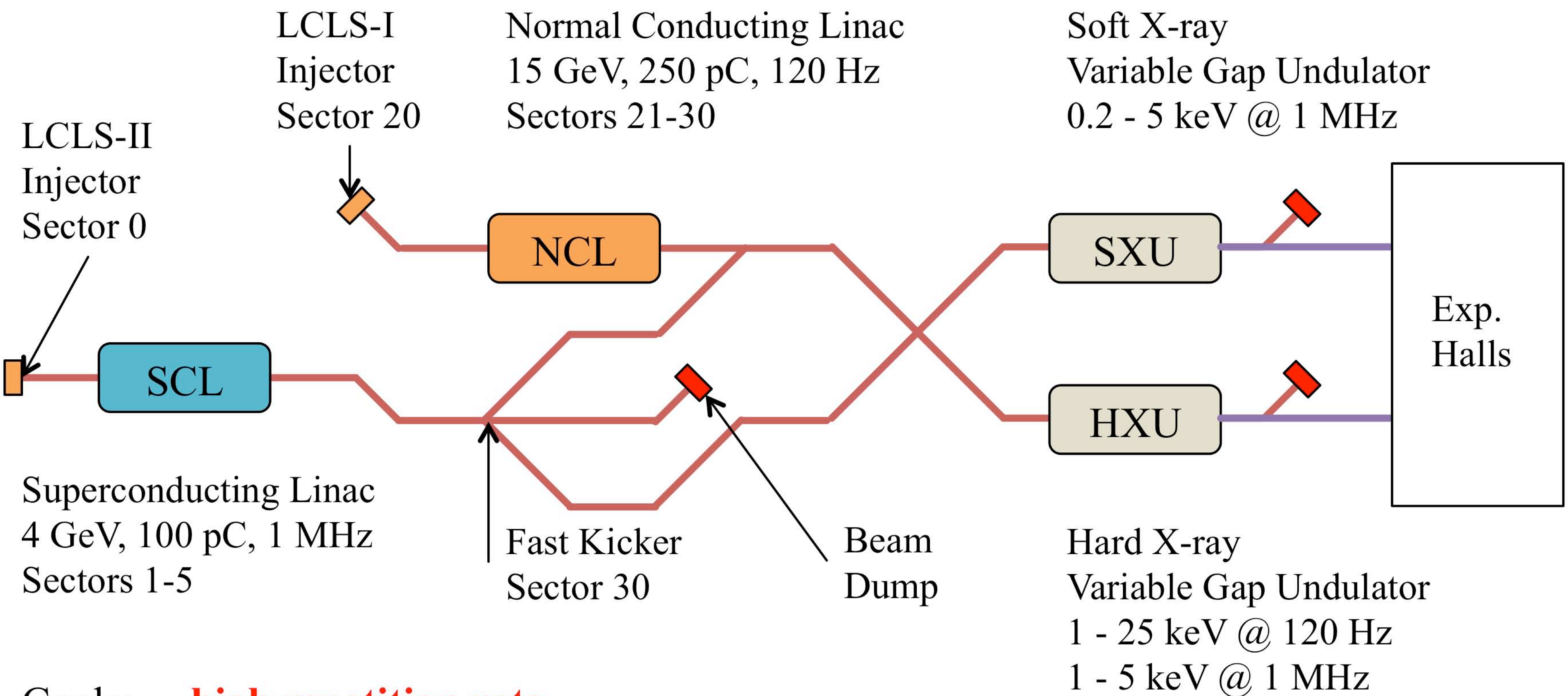

Goals: **high repetition rate**
large spectral range
spectral tunability
increased coherence

needed capabilities were outlined in the July 2013 BESAC report

LCLS-II Injector Specifications

Injector	Electron energy	[MeV]	98	
	Repetition rate	[MHz]	0.929	
	Dark current	[nA]	< 400	
	Bunch charge	[pC]	100, 10 - 300	
	Peak current	[A]	12, 4 - 50	
	Normalized slice emittance	[rms, μm, 95%]	0.4, 0.2 - 0.6	
	Bunch length	[rms, mm]	0.3 - 10	
	Slice energy spread	[rms, keV]	1 - 5	
Gun	* APEX VHF gun, next slide			
Photocathode	**Quantum Efficiency**	[%]	**> 0.5**	Cs_2Te conservative baseline
	Intrinsic Emittance	[μm/mm]	**< 1**	
	Lifetime	[days]	**> 10**	
Lasers (x2)	IR Power	[W]	50	commercial systems available
	UV Energy @ Photocathode	[μJ]	0.3	
	IR Energy @ Laser Heater	[μJ]	15	

APEX: VHF Normal Conducting CW RF Gun

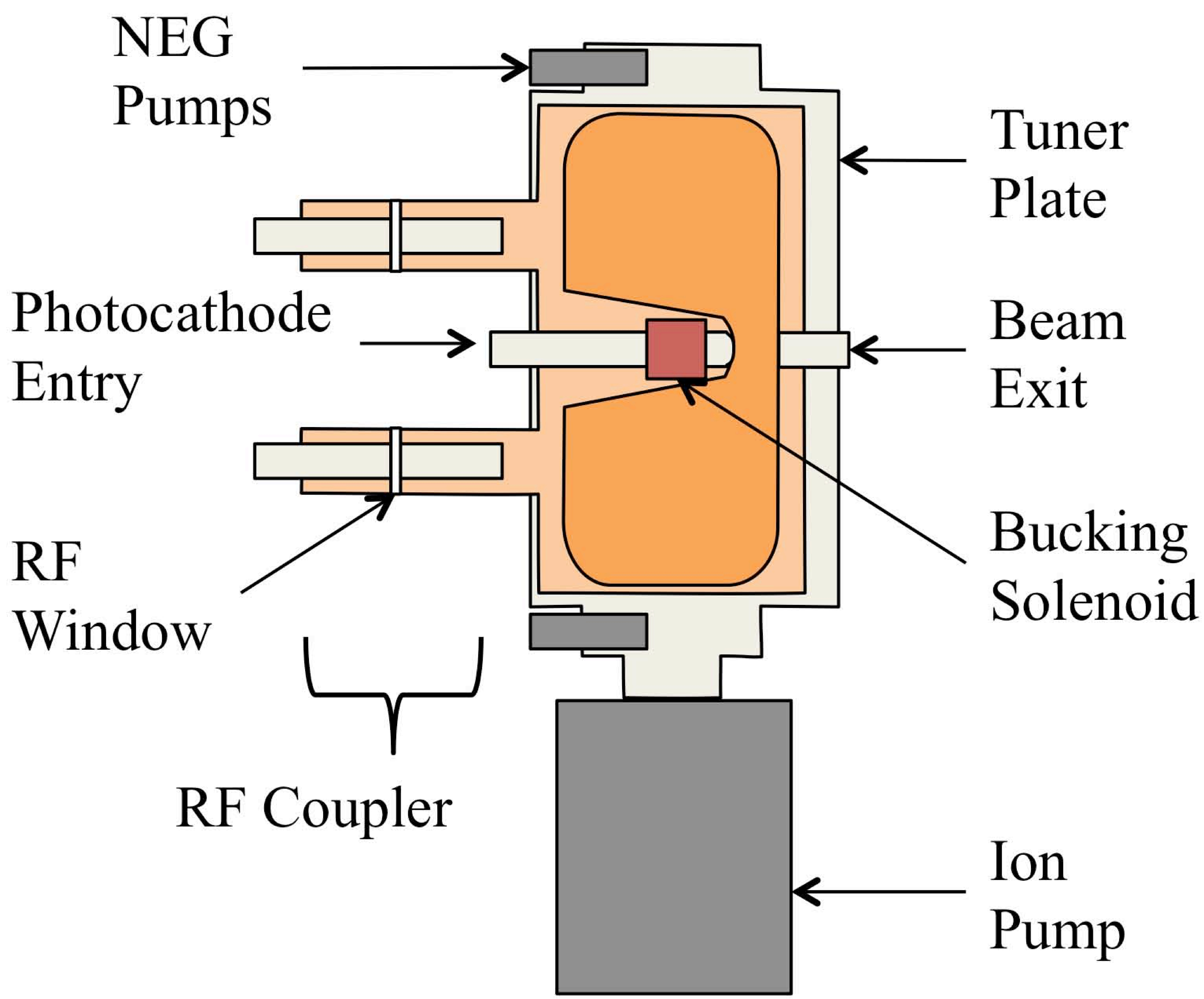

APEX: the Advanced Photoinjector Experiment

Frequency	186 MHz
Field @ cathode	19.5 MV/m
Accelerating gap	4 cm
Vacuum w/ RF	$< 6 \times 10^{-10}$ torr
Vacuum w/o RF	$1 - 5 \times 10^{-11}$ torr

K. Baptiste, et al, NIM A 599, 9 (2009)
F. Sannibale, et al., PRST-AB 15, 103501 (2012)

large cavity → withstand CW heat load at high gradient

large apertures → high vacuum conductivity, semiconductor photocathodes

NC technology → reliability

LCLS-II Injector Layout

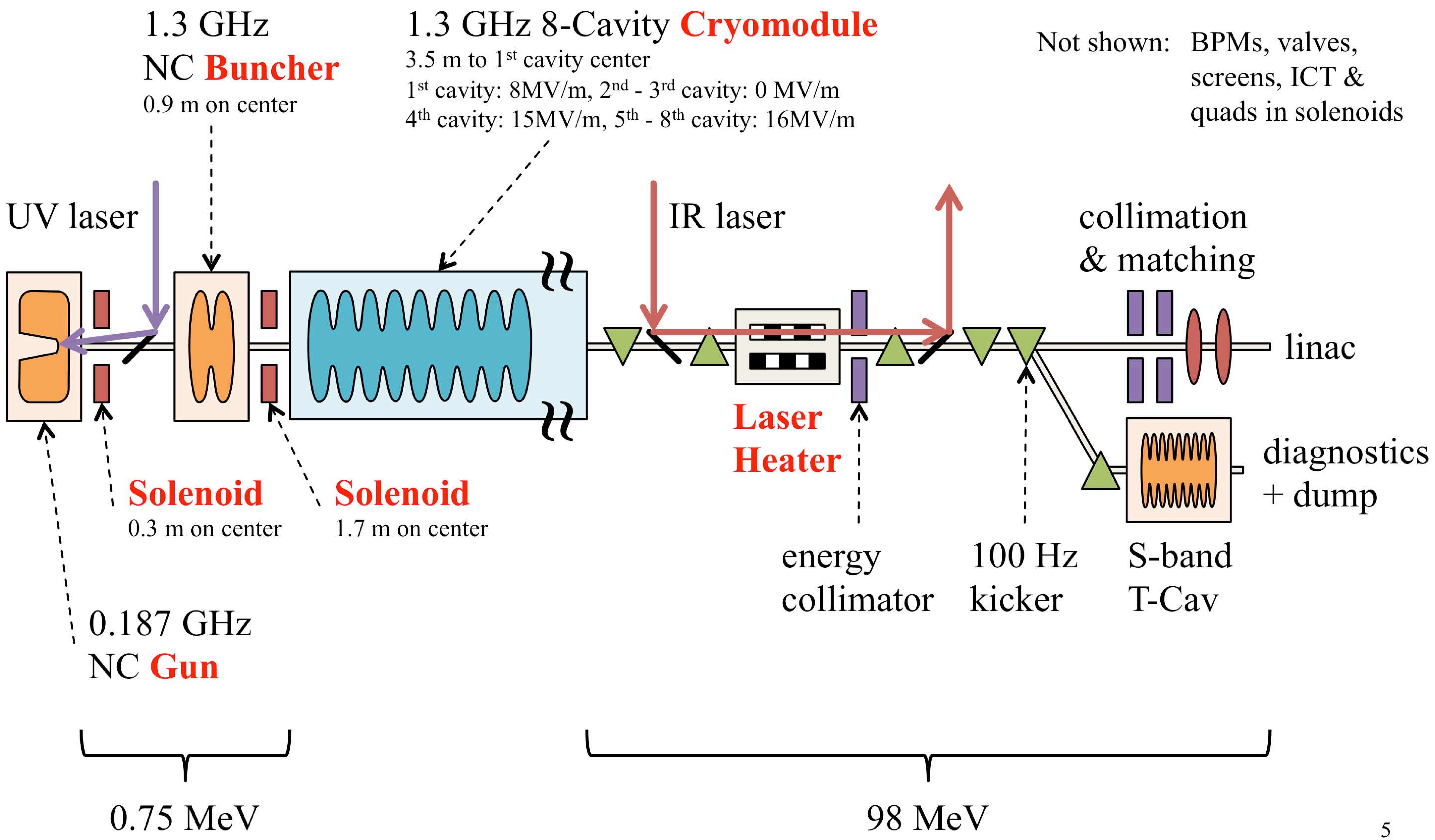

LCLS-II Injector Simulations

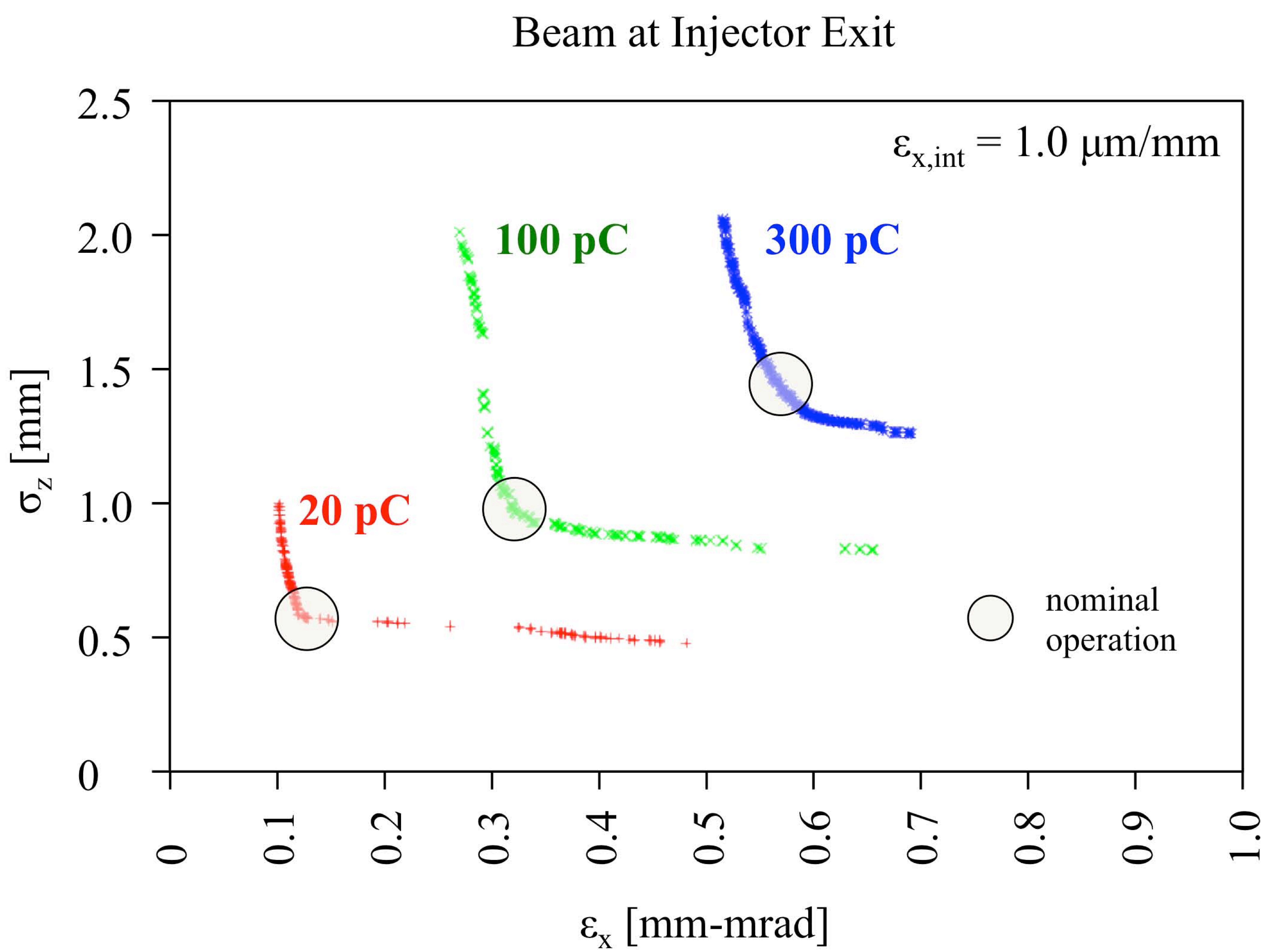

layout optimized by simulation

LCLS-II Injector Commissioning Timeline

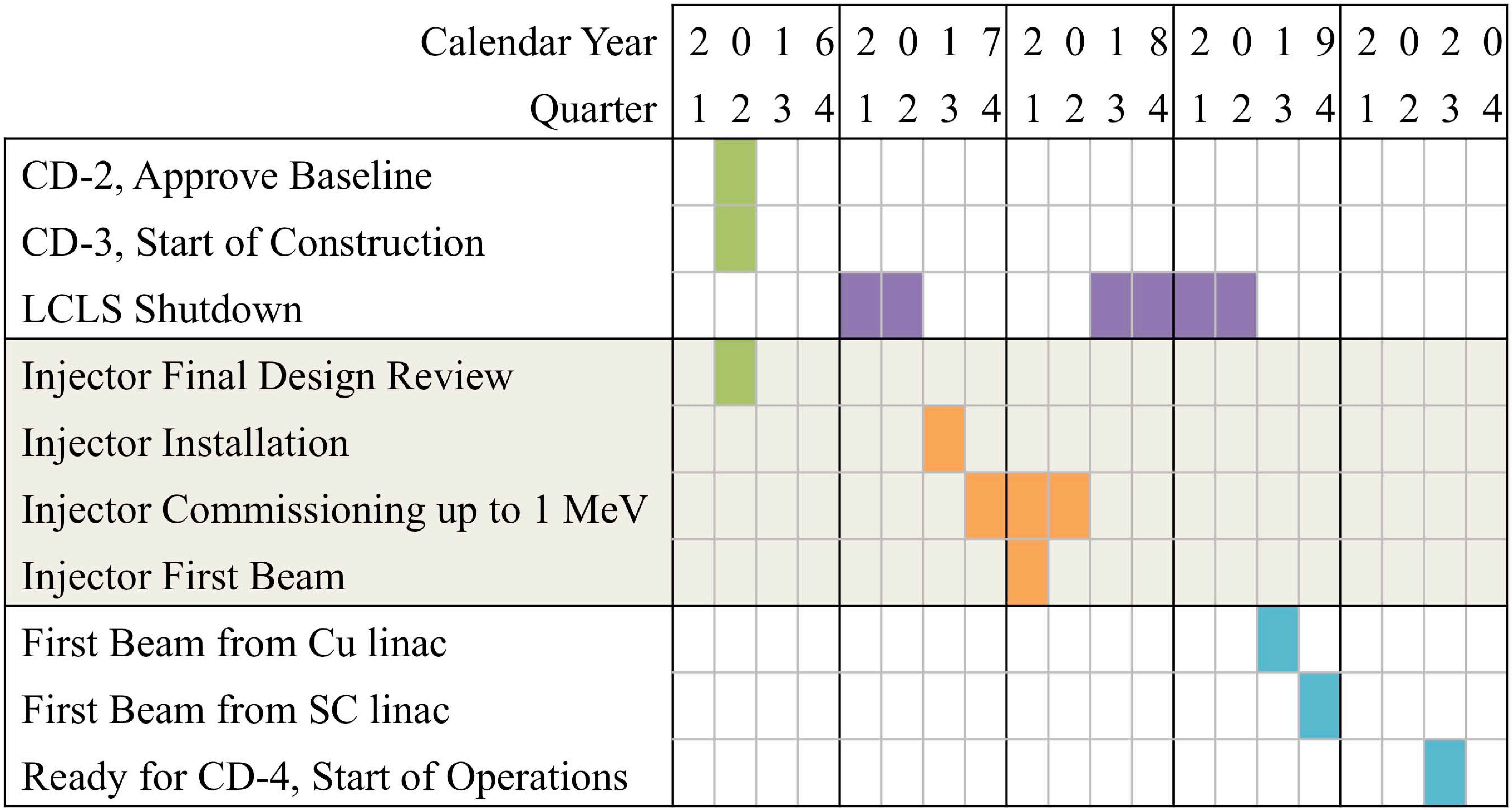

SLAC - LBNL Collaboration


Daniele Filippetto


Houjun Qian

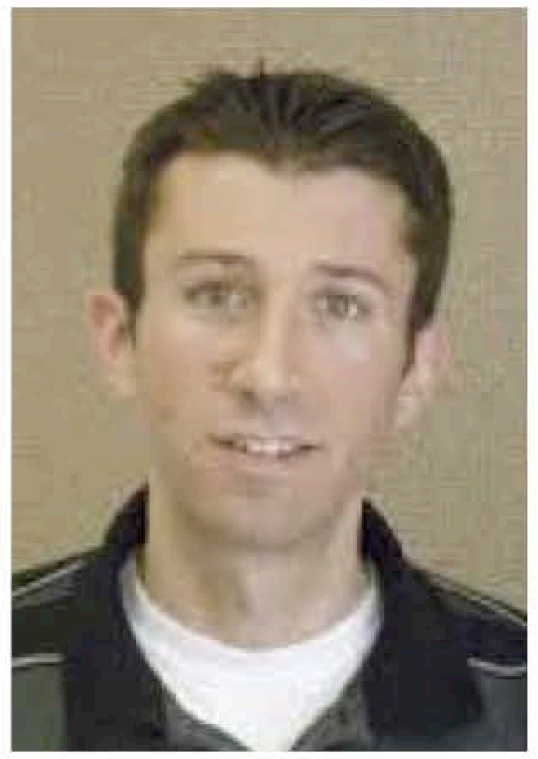
Chad Mitchell


Fernando Sannibale


Feng Zhou

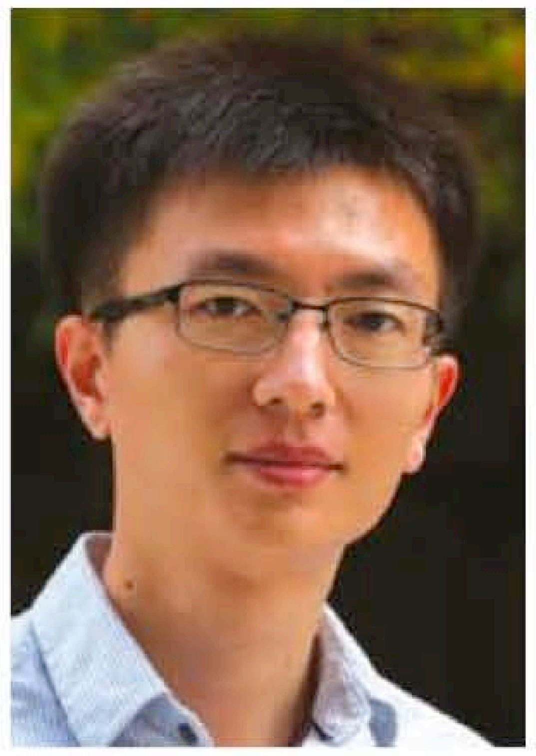
Renkai Li

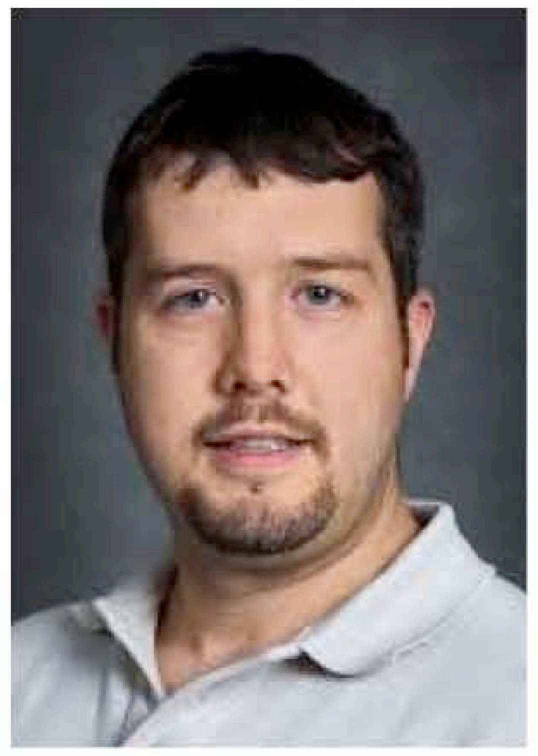
Theo Vecchione


Stephen Giermann


John Schmerge

APEX provides SLAC a great opportunity to work w/ the future LCLS-II gun

Already results are good, but complete optimization is an incremental process requiring careful systematic characterization → **collaborative efforts will continue**

APEX colleagues not pictured above:

K. Baptiste, C. Cork, S. De Santis, M. Dickinson, L. Doolittle, J. Doyle, J. Feng, G. Harris, G. Huang, H. Huang, R. Huang, M. Johnson, M. Jones, T. Kramasz, S. Kwiatkowski, D. Leitner, R. Lellinger, V. Moroz, W. E. Norum, H. Padmore, G. Portmann, J. Staples, D. Syversrud, M. Vinco, S. Virostek, W. Wan, R. Wells, M. Zolotorev, …

APEX Layout

Phase-II diagnostics:

Quad 1 & 3 + T-Cav + Screen 3 → **Slice emittance**

Hor. & ver. slits + Screen 2 → Hor. & ver. **projected emittance**

Spectrometer Dipole & Screen → **Energy & Energy spread**

T-Cav + Screen 3 → **Bunch length**

APEX Results

	Deliverable		Required	Measured
1.)	**vacuum** compliance [2]			
	pressures in gun without RF	[torr]		2×10^{-11}
	pressures in gun with nominal RF	[torr]		$3\text{-}5 \times 10^{-10}$
2.)	**dark current** compliance [1]	[nA]	< 400	0.1
3.)	**continuous operation at nominal power** [2]	[hours]	> 24	yes
	nominal beam energy	[keV]	750	> 840
4.)	**photocathode performance and reliability** [3]			
	intrinsic emittance of Cs_2Te	[µm/mm]	< 1	0.7
	lifetime of Cs_2Te	[days]	> 10	17
5.)	**high-brightness from injector based on VHF Gun**			
	charge per bunch	[pC]	≥ 20 pC	20 - 25
	peak current	[A]	≥ 5	5 - 9
	emittance (smaller w/o space charge effects)	[µm]	≤ 0.25	~ 0.25
	slice energy spread (smaller at higher energies)	[keV]	≤ 15	< 9

1.) R. Huang, et al., PRST-AB 18, 013401 (2015)
2.) F. Sannibale, et al., PRST-AB 15, 103501 (2012)
3.) D. Filippetto, et al., APL 107, 042104 (2015).

Projected Emittance Measurement

K_2CsSb, 20 pC, 15.7 MeV, 6.5 A peak, Laser: σ_x = 170 µm, σ_y = 173 µm, 28 ps

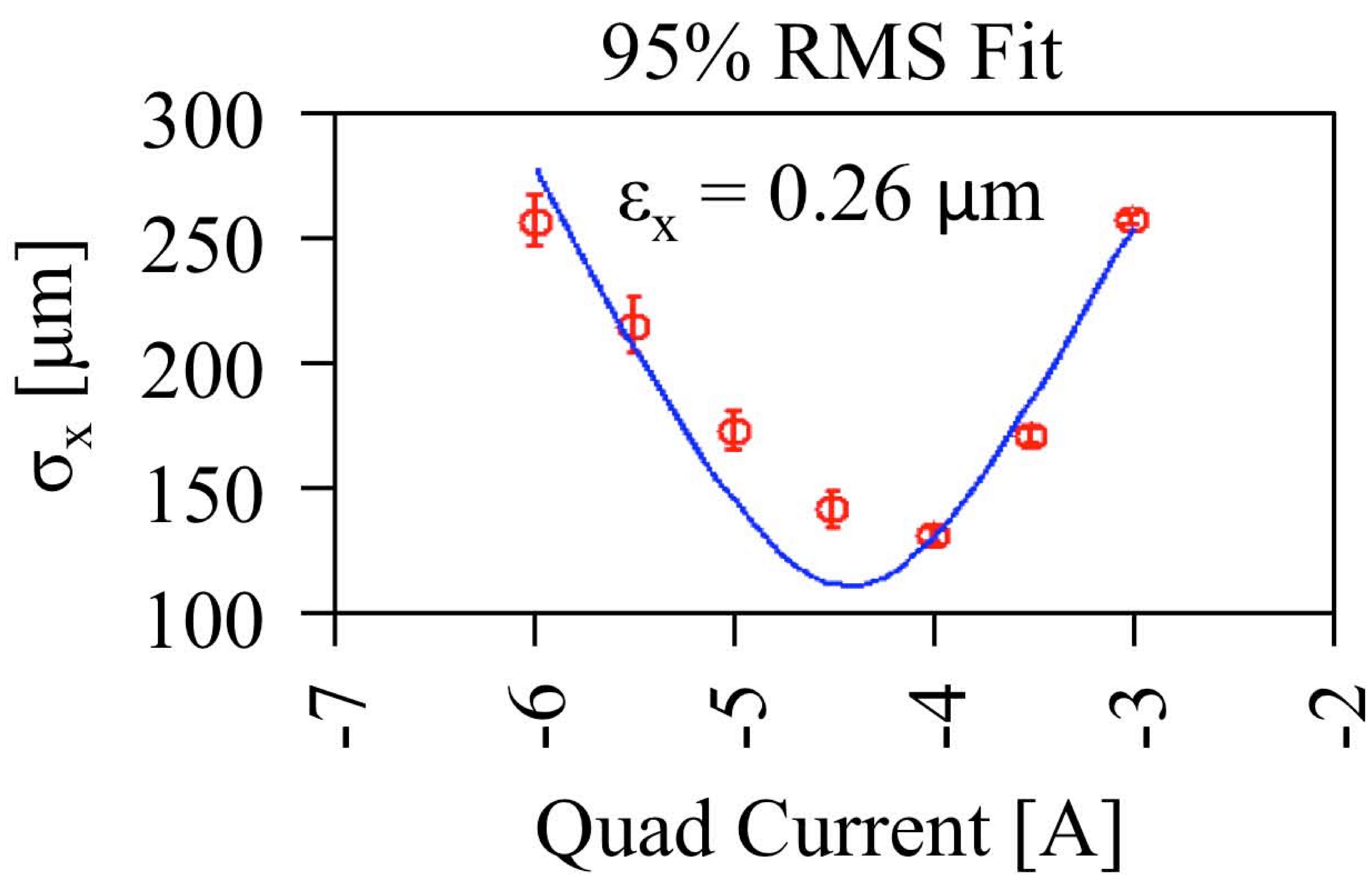

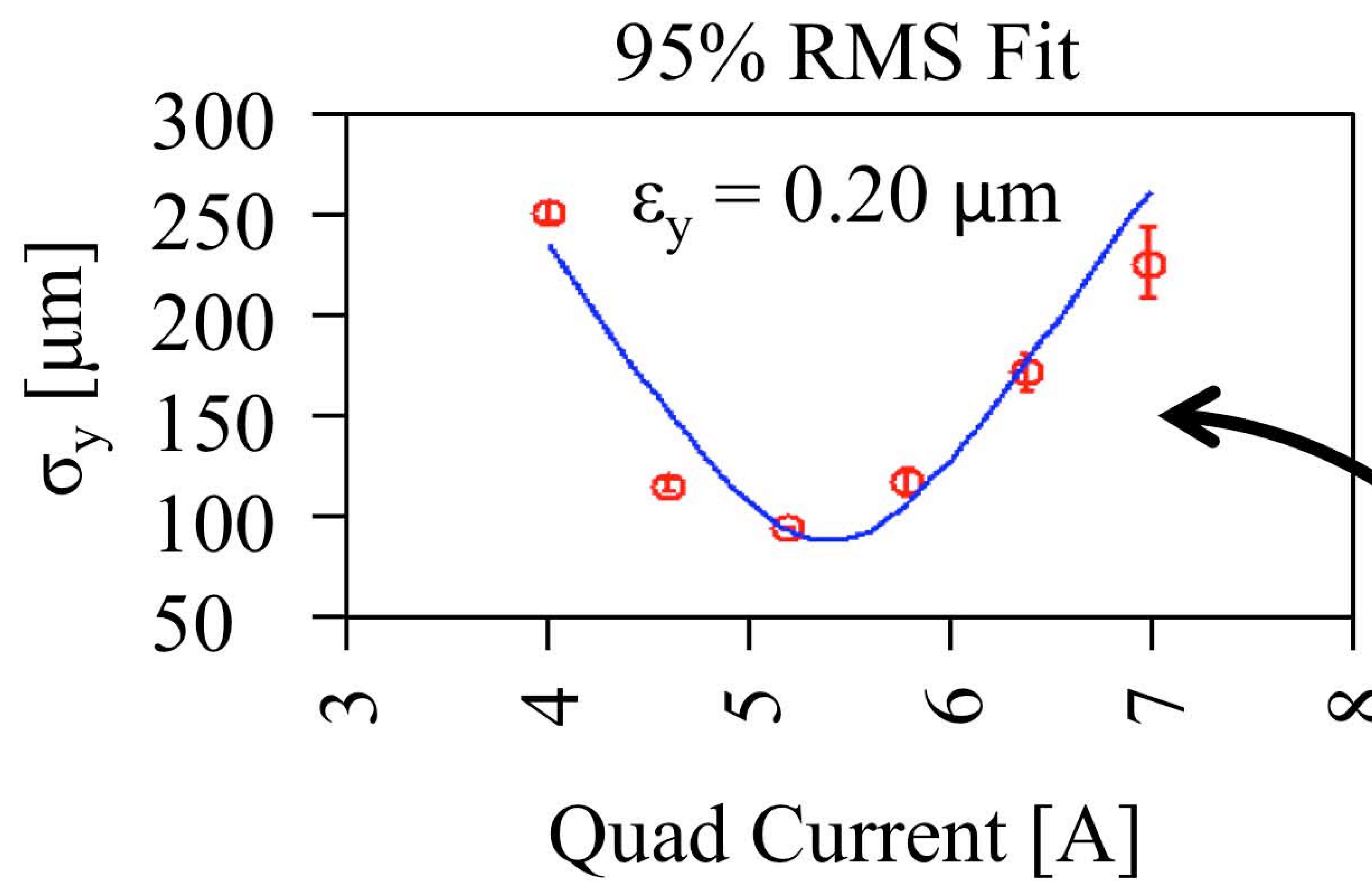

diff fits same data

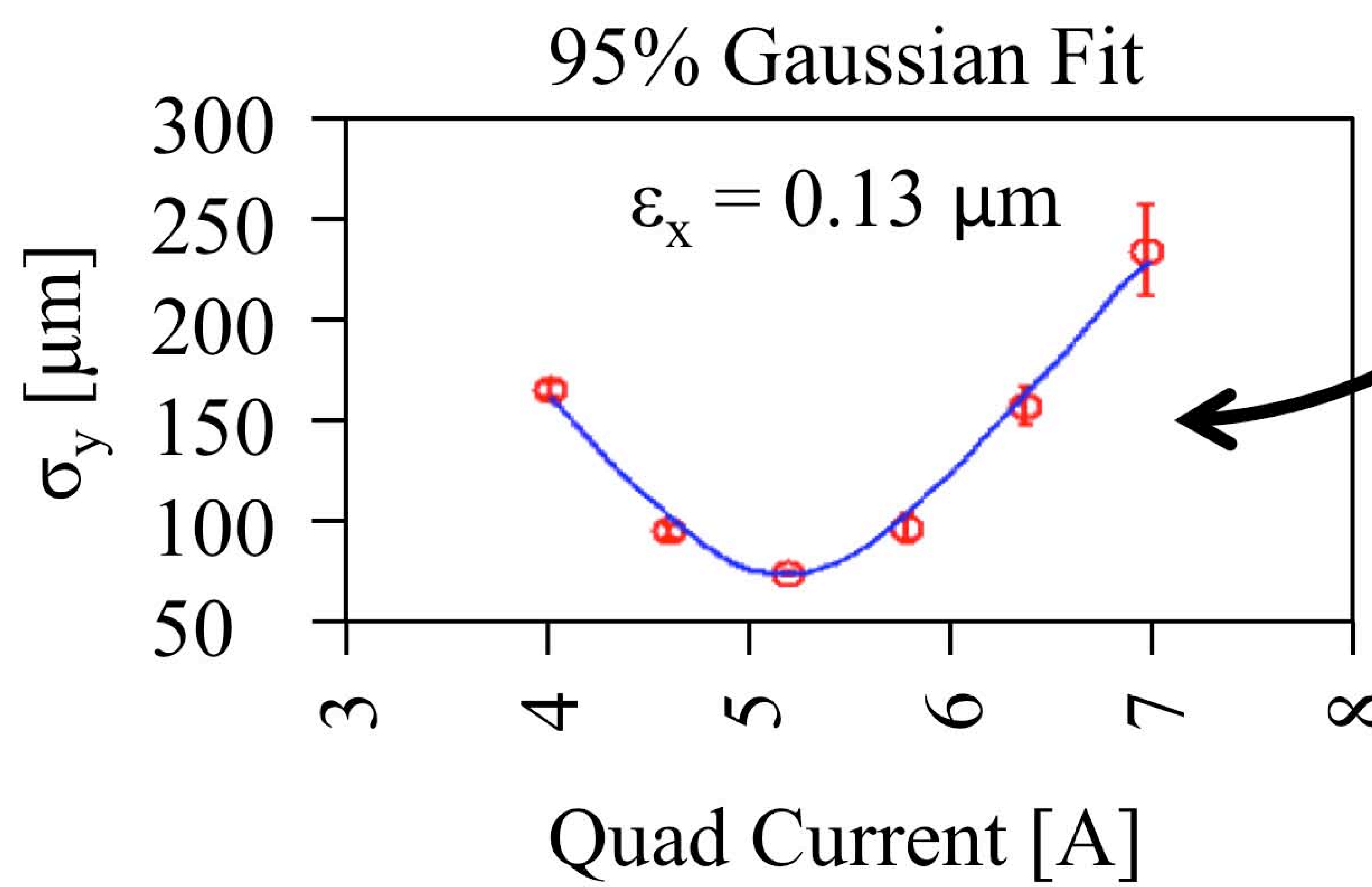

compares well w/ LCLS-II spec.
although value may be an overestimate

working on improving laser profile
both longitudinal + transverse

simulations match results
gives confidence to numerical methods

Lessons Learned: Reducing Dark Current

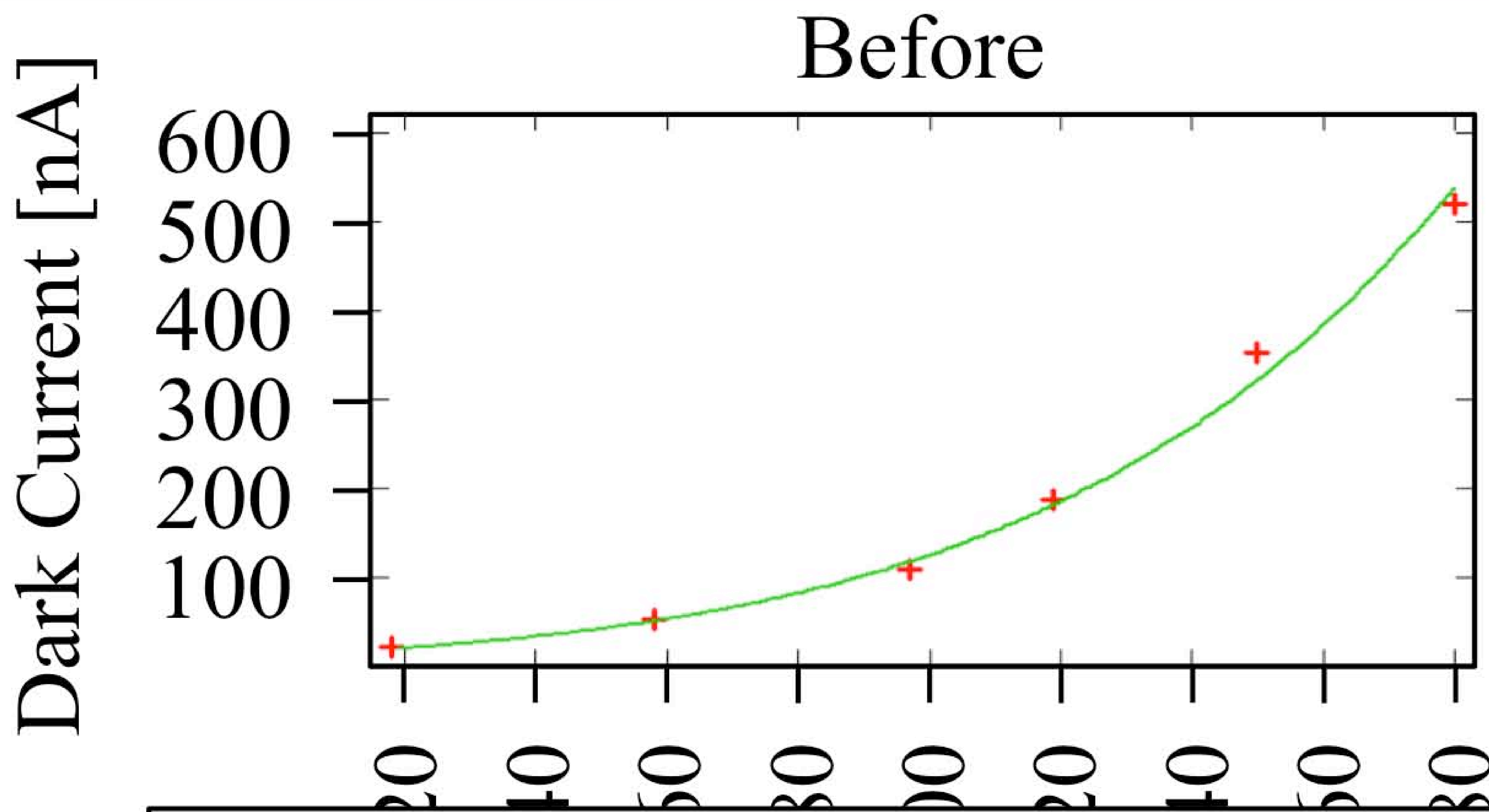

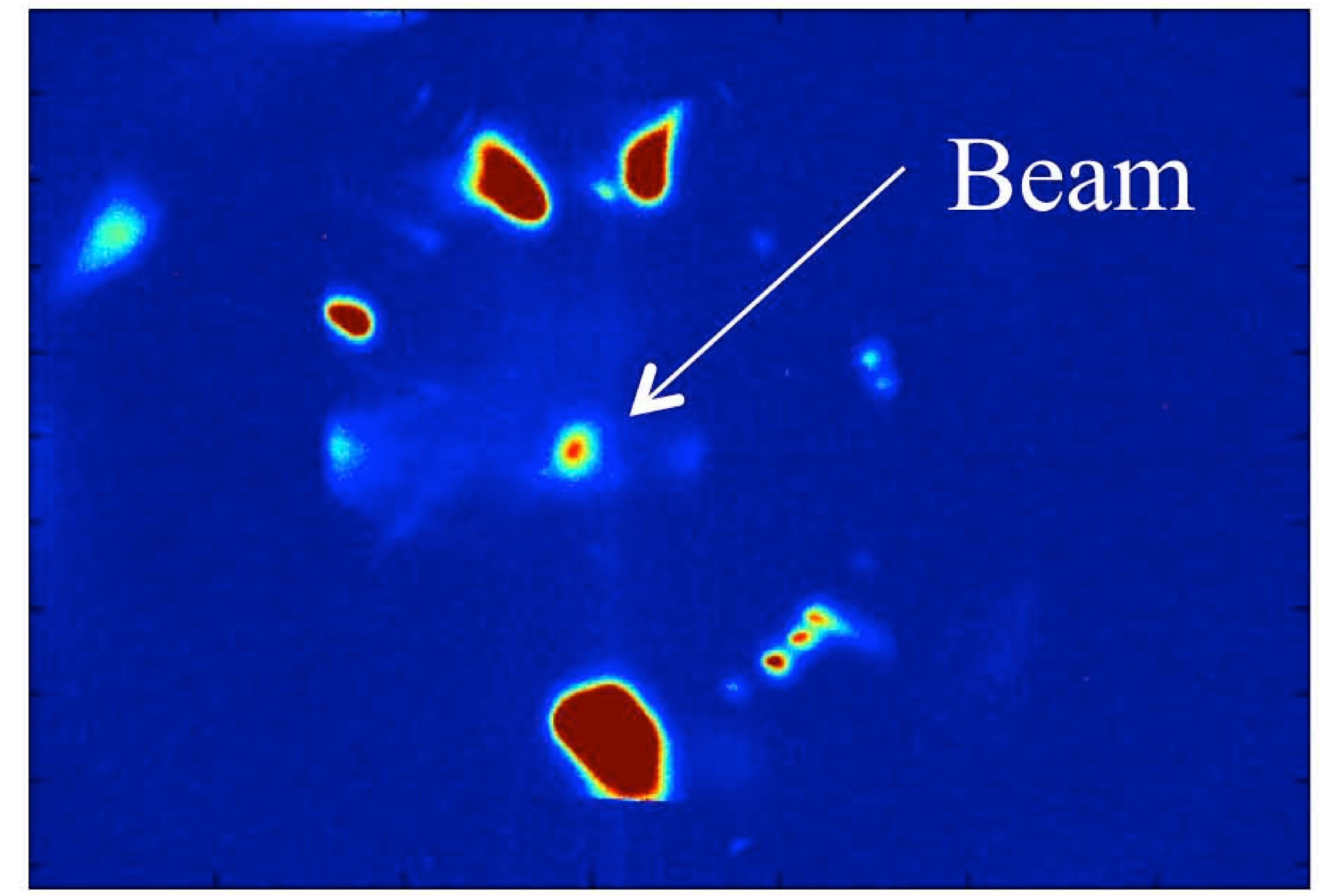

Mirror polishing and dry ice cleaning → > 3-orders of magnitude reduction

350 nA @ 750 keV

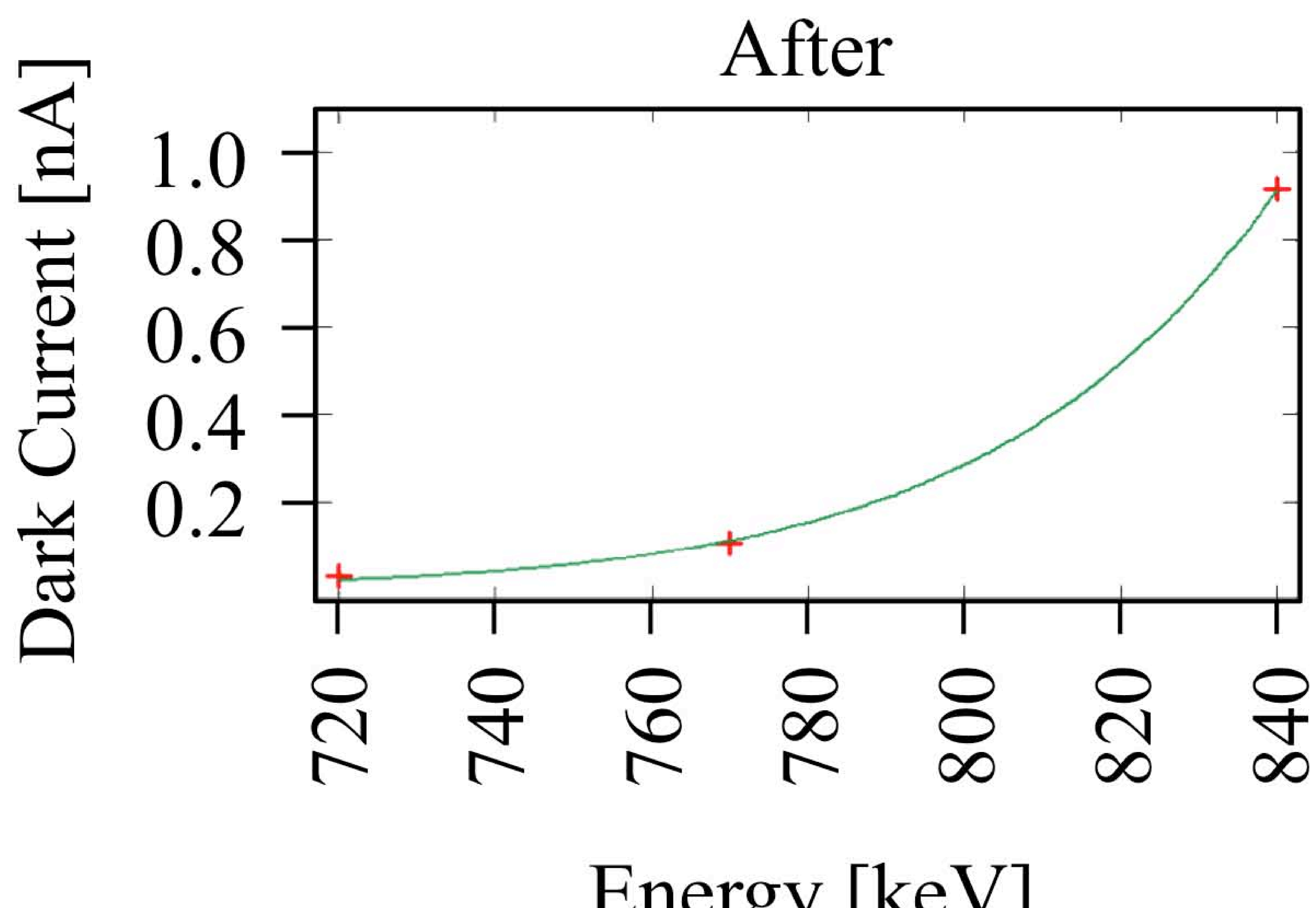

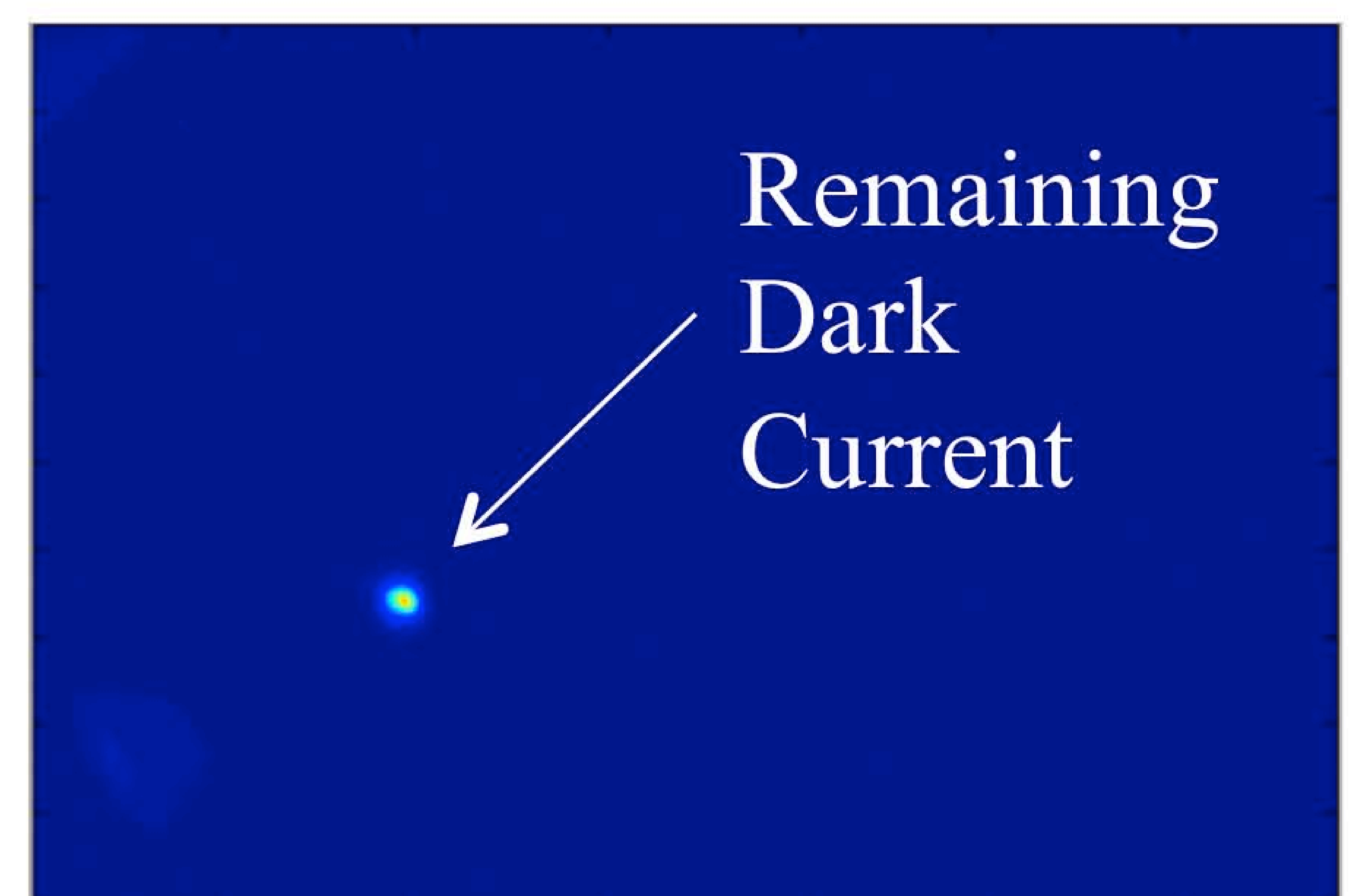

0.1 nA @ 750 keV

Lessons Learned: Avoid RF Window Charging

during high power operation a small vacuum leak was observed in one of the RF couplers ($7 \times 10^{-11} \rightarrow 8 \times 10^{-10}$ torr)

Visual inspection showed evidence of a "puncture", presumably due to charge pile-up on the ceramic window

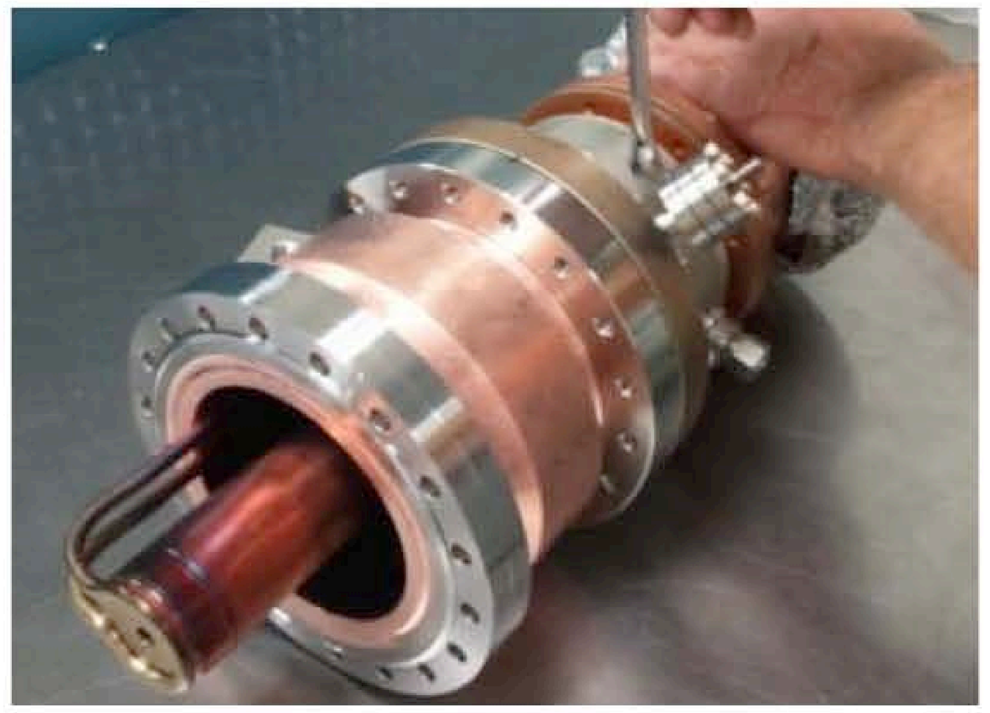

Simulations indicated field emission from particulates inside the gun cavity as the source for the electrons.

Steps are being taken to prevent a recurrence

1.) Elbow added to remove any line of sight between the gun cavity and the ceramic windows

2.) Shielding added to prevent x-rays to get on the RF window.

3.) Thicker TiN coating on the RF coupler coppers wall to prevent multipacting. If necessary, solenoids in the area can be installed.

CW operation to resume after the new RF window is installed

APEX Photocathode Performance

		LCLS-II baseline	Photocathode Cs_2Te on Mo [1] INFN-LASA	K_2CsSb on Mo LBNL
vacuum requirement	[torr]		10^{-9}	10^{-10}
drive laser wavelength	[nm]		263	526
diameter of emitting area	[mm]		5	10
photocathode film thickness	[nm]		80	100 nm
maximum repetition rate used so far	[Hz]		1×10^6	10, 1 MHz soon
maximum pulse charge extracted so far	[pC]		> 500	> 500
initial **QE**	[%]		**> 10**	**≤ 8**
intrinisc emittance @ 500 fC	[µm/mm RMS]		**0.7 - 0.8**	**< 0.60**
temporal response	[ps]		< 1	< 1
1/e lifetime	[hrs/Langmuirs]		400/15	measurement soon
service life (10% to 0.5% QE)	[days]		50	measurement soon
storage life in suitcase	[days]		∞	> 30

1.) D. Filippetto, et al., APL 107, 042104 (2015).

FEL Performance Depends on Emittance

Ming Xie model [1,2] is useful to illustrate this dependence

gives radiated power as a function of the FEL parameter, ρ, which in turn depends implicitly on emittance, ε_x, through σ_x.

$$\rho[\varepsilon_x] = \left(\left(\frac{I}{I_A}\right) \left(\frac{\lambda_u}{2\pi\sigma_x[\varepsilon_x]}\right)^2 \left(\frac{K}{\sqrt{2}}\left(J_0\left[\frac{K^2}{4+2K^2}\right] - J_1\left[\frac{K^2}{4+2K^2}\right]\right)\right)^2 \left(\frac{1}{2\gamma}\right)^3 \right)^{1/3}$$

Benefits of reducing emittance:

increased photon pulse energy
extension of the accessible spectral range
increased degree of transverse coherence
building shorter undulators saves money

1.) M. Xie, Proc. of the 1995 Particle Accelerator Conf., Dallas, USA, 183-185.
2.) Z. Huang and K. J. Kim, *PRSTAB* **10**(3), 034801 (2007).

Emittance Reduction Creates New Possabilities

LCLS-II design specification: 0.4-µm emittance at 100-pC, <100-fs rms electron bunches

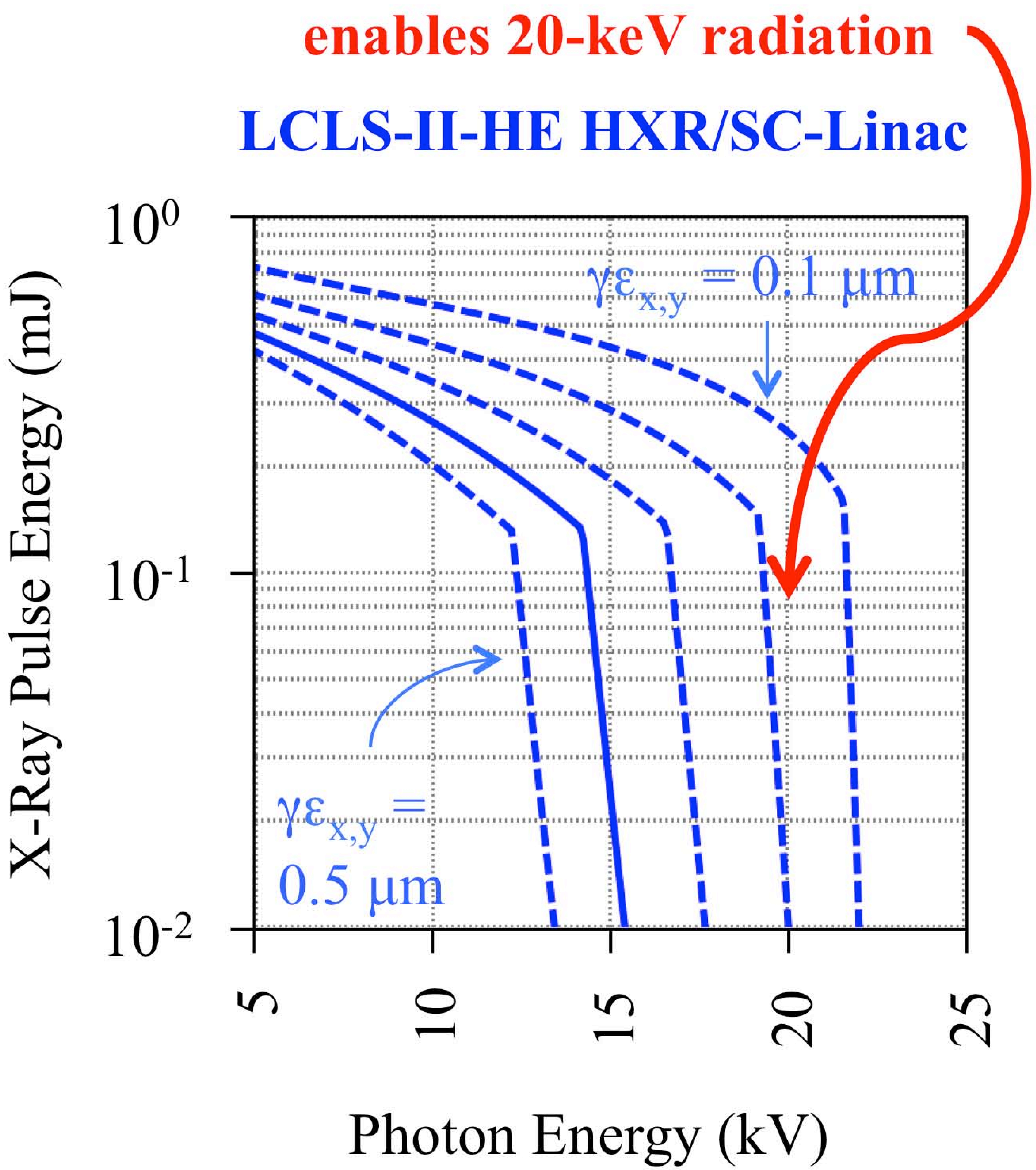

I_{pk}	= 1 kA	E	= 8 GeV
Q	= 100 pC	σ_E	= 0.5 MeV
L_u	= 140 m	$\langle\beta_{x,y}\rangle$	= 20 m
λ_u	= 26 mm	p_f	= 0.8

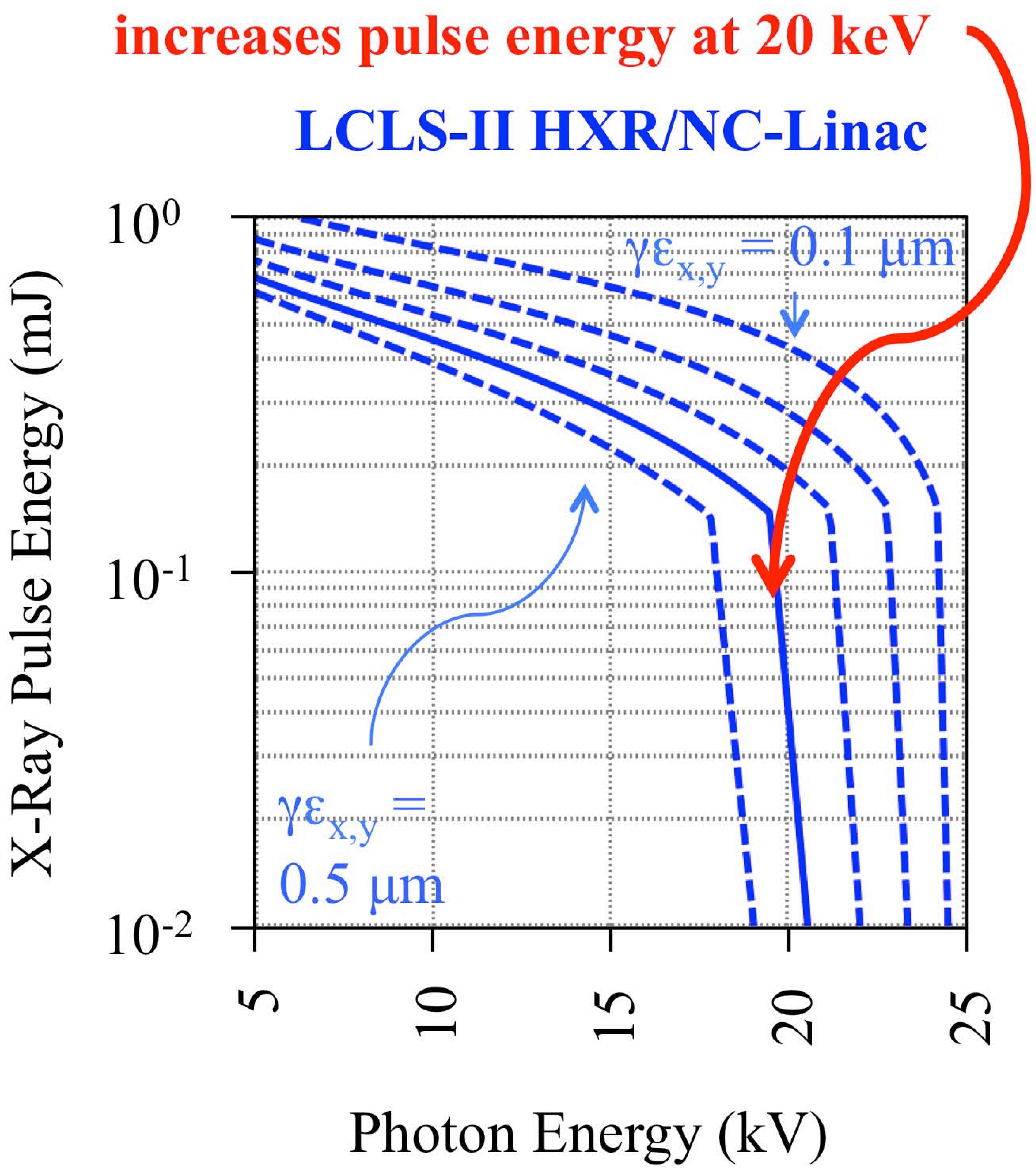

I_{pk}	= 3.5 kA	E	= 8.4 GeV
Q	= 100 pC	σ_E	= 1.5 MeV
L_u	= 140 m	$\langle\beta_{x,y}\rangle$	= 30 m
λ_u	= 26 mm	p_f	= 0.8

Reducing Photocathode Emittance

Change laser wavelength

$$\varepsilon_n \approx \sigma_{x,y}\sqrt{\frac{\hbar\omega - \phi + \Delta\phi}{3mc^2}} \quad \text{vs} \quad QE \propto \left(\frac{\hbar\omega - \phi + \Delta\phi}{kT}\right)^2$$

Change drive laser angle of incidence & polarization

D. Xiang et al., *NIMA* **562**(1), 48-52 (2006).

Change extraction field and phase

$$\Delta\phi = \sqrt{\frac{eF}{4\pi\varepsilon_0}}$$

Operate at reduce temperature

$$\varepsilon_n = \sigma_{x,y}\sqrt{\frac{kT}{mc^2}} \longleftarrow \text{thermal limit}$$

L. Cultrera et al., *PRSTAB* **18**(11), 113401 (2015).

Reduce surface roughness < a few nm

H. J. Qian et al., *PRSTAB* **15**(4), 040102 (2012).

Use surface coatings to either protect or enhance the emitting surface

*recent conference proceedings

Excite surface state emission

$$m^*_{surf} > m$$

E. Pedersoli et al., *APL* **93**(18), 183505 (2008).

Use nano-engineered surfaces to improve photocathode optical absorption

A. Polyakov et al., *JVSTB* **29**(6), 06FF01 (2011).

Use oriented single crystals

T. Li, B. L. Rickman and W. A. Schroeder, *PRSTAB* **18**(7), 073401 (2015).
T. Li, B. L. Rickman and W. A. Schroeder, *JAP* **117**(13), 134901 (2015).

Multilayer "designer" photocathodes

D. Velázquez et al., *App Surf Sci* **360**, 762-766 (2016).

Analytical Photoemission Model

$$\varepsilon_n = \sigma_{x,y}\sqrt{\frac{kT}{mc^2}}\sqrt{\frac{Li_3\left[-Exp\left[\frac{\hbar\omega-\phi+\Delta\phi}{kT}\right]\right]}{Li_2\left[-Exp\left[\frac{\hbar\omega-\phi+\Delta\phi}{kT}\right]\right]}}$$

reduces to D-S

$$\varepsilon_n \approx \sigma_{x,y}\sqrt{\frac{\hbar\omega-\phi+\Delta\phi}{3mc^2}}$$

but more accurate when $\hbar\omega \approx \phi_{\text{eff}}$

$$QE \propto Li_2\left[-Exp\left[\frac{\hbar\omega-\phi+\Delta\phi}{kT}\right]\right]$$

reduces to D-S

$$QE \propto \left(\frac{\hbar\omega-\phi+\Delta\phi}{kT}\right)^2$$

Sommerfeld free electron model

Electronic states and occupational probabilities

1.) Electrons bound by uniform potential

2.) Constant density of states

3.) Occupation governed by Fermi-Dirac statistics

All surfaces treated identically

Spicer 3-step emission model

Identifies a sequence of steps in photoemission

1.) Electrons absorb photons, ΔE normal to surface

2.) Electrons diffuse to surface

3.) Electrons escape, ΔE = μ+ϕ-ħω normal to surface

D. Dowell and J. Schmerge, *PRSTAB* **12**(11), 074201 (2009).
T. Vecchione et al., Proc. of the 2013 International FEL Conf., Manhattan, USA, TUPSO83.

Photocathodes can be rather complex though…

Copper photocathode

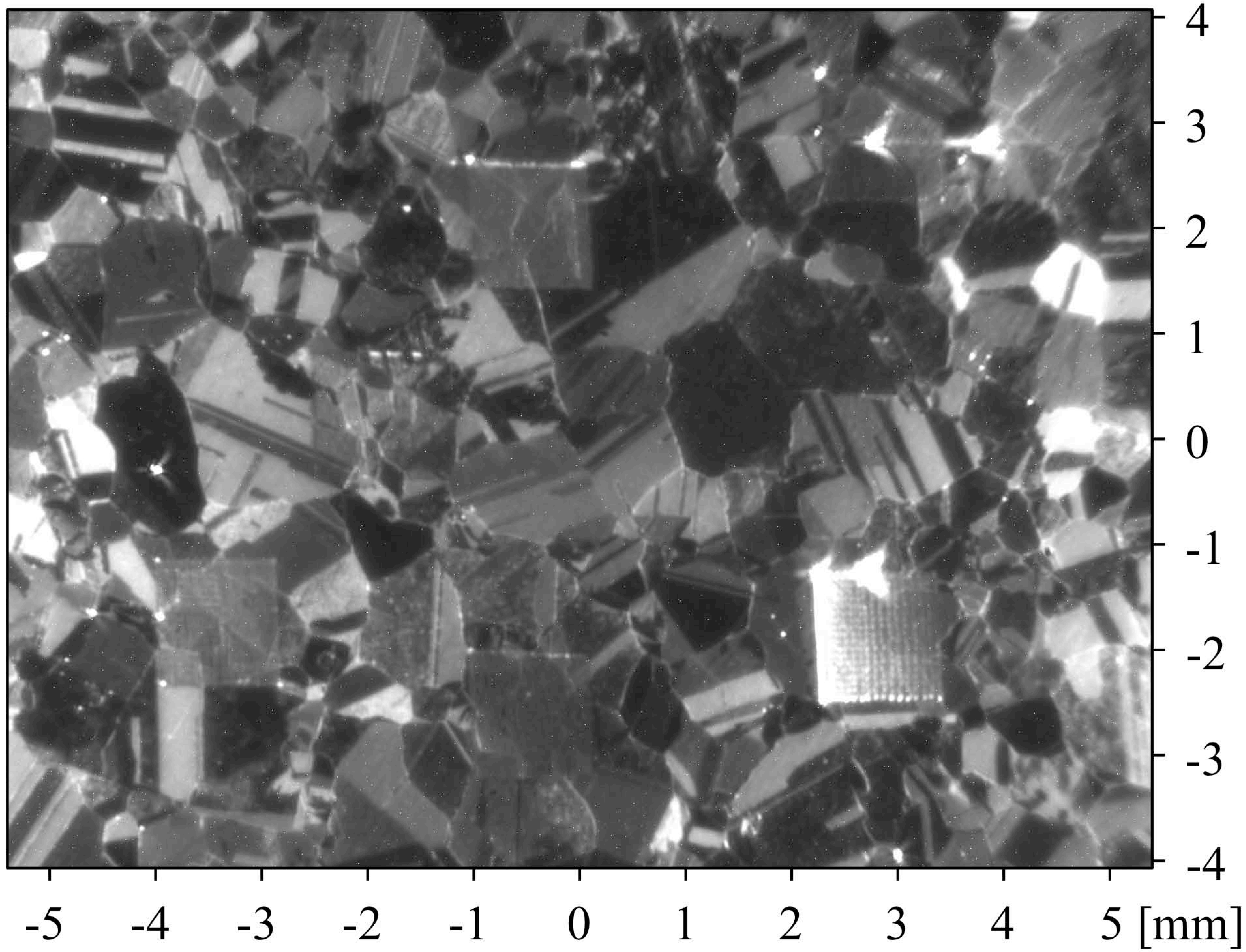

Density-Functional Theory (DFT)

DFT is a widely accepted technique for calculating ground state electronic structure
Basis: N-body Schrödinger equation → equivalent N, Kohn-Sham 1-body equations

$$\left(-\frac{1}{2}\nabla_i^2+\frac{1}{2}\int\frac{n(r')}{|r-r'|}dr'-\sum_I\int\frac{Z_I n(r')}{|r'-R_I|}dr'+\frac{1}{2}\sum_{I\neq J}\frac{Z_I Z_J}{|R_I-R_J|}+\varepsilon_{xc}\left[n(r)\right]\right)\psi_i(r)=\varepsilon_i\psi_i(r)$$

“exchange-correlation” term is defined to be anything such that the equivalency true

P. Hohenberg and W. Kohn, *Phys Rev* **136**, B864 (1964).
W. Kohn and L.J. Sham, *Phys Rev* **140**, A1133 (1965).

Calculations can be done using a freely distributed software package, ABINIT

1.) Plane wave basis set & periodic boundary conditions

2.) Ion cores replaced w/ Troullier-Martins type norm-conserving pseudopotentials

3.) Exchange-correlation is given by a LDA Teter-Pade parameterization

4.) Surface electronic structure calculated using slab supercells

Including Electronic Structure in a Photoemission Model

Approach: Use DFT to calculate photocathode electronic structure

Include results as a supply function is a 1-step photoemission model

Model: Brillouin zone populated by interpolating between DFT eigenstates

K-space is searched until enough occupied states with sufficient energy and momentum for emission are found.

States undergo excitation and emission similar to the analytical model

The model can be extended to include the effects of finite temperatures, work function shifts in the presence of surface dipole layers and having separate contributions from surface states.

Goal: Identify photocathodes that emit with minimal emittance at a given charge

Applies to both metals for the LCLS-I & to semiconductors for the LCLS-II

Findings should guide future work → improved machine performance

Verifying Emission Simulations Using ARPES Data

Simulations

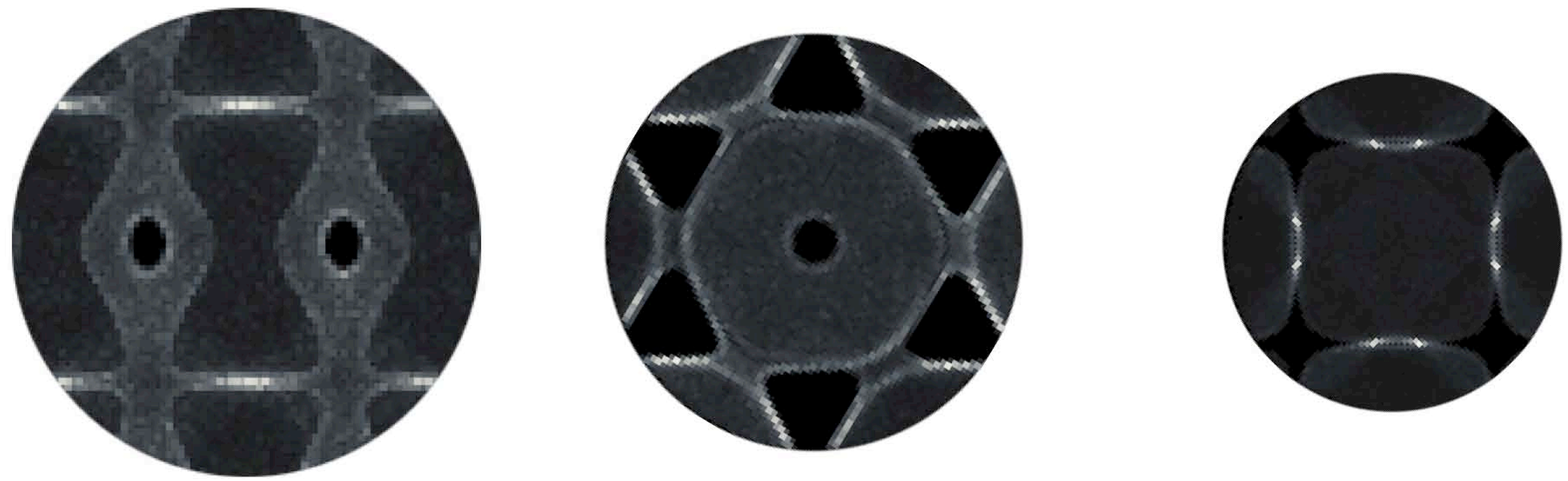

ħω = 21.2 eV
ΔE = 0.1 eV

(100) (111) (110)

Experiments

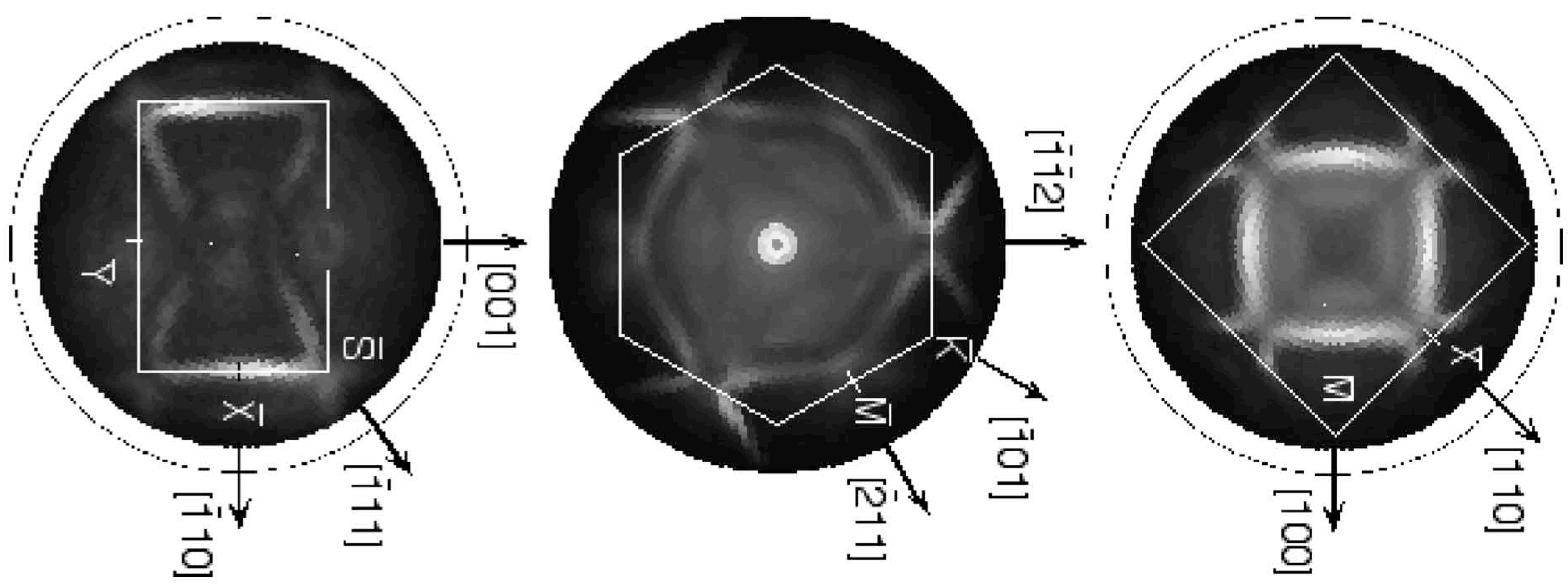

Pretty good agreement

Reproduced from P. Aebi et al., *Surf. Sci.* **307**, 917-921 (1994).

Results Match Published Experimental Work

Surface work function calculations done using a slab supercell geometry

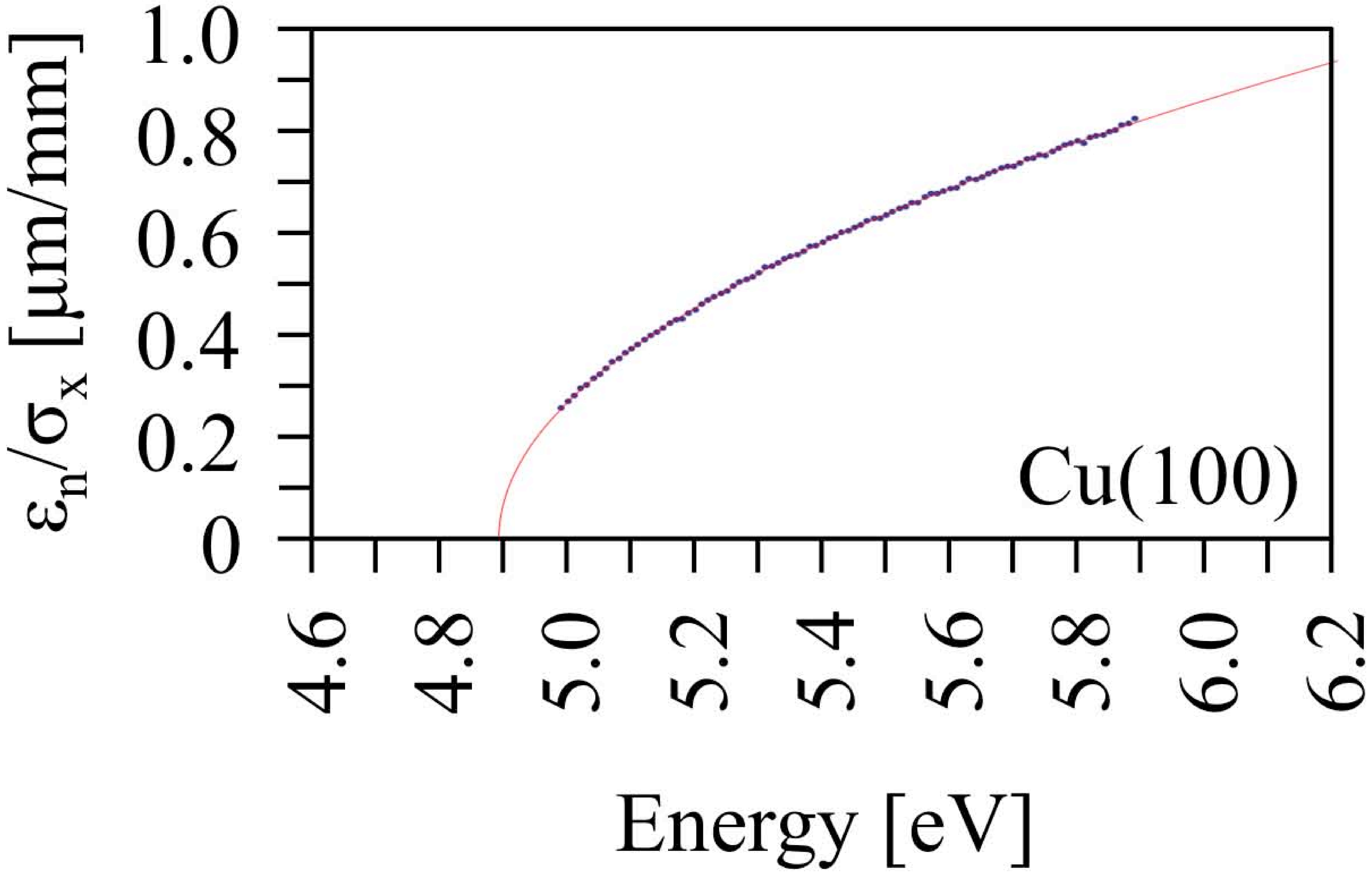

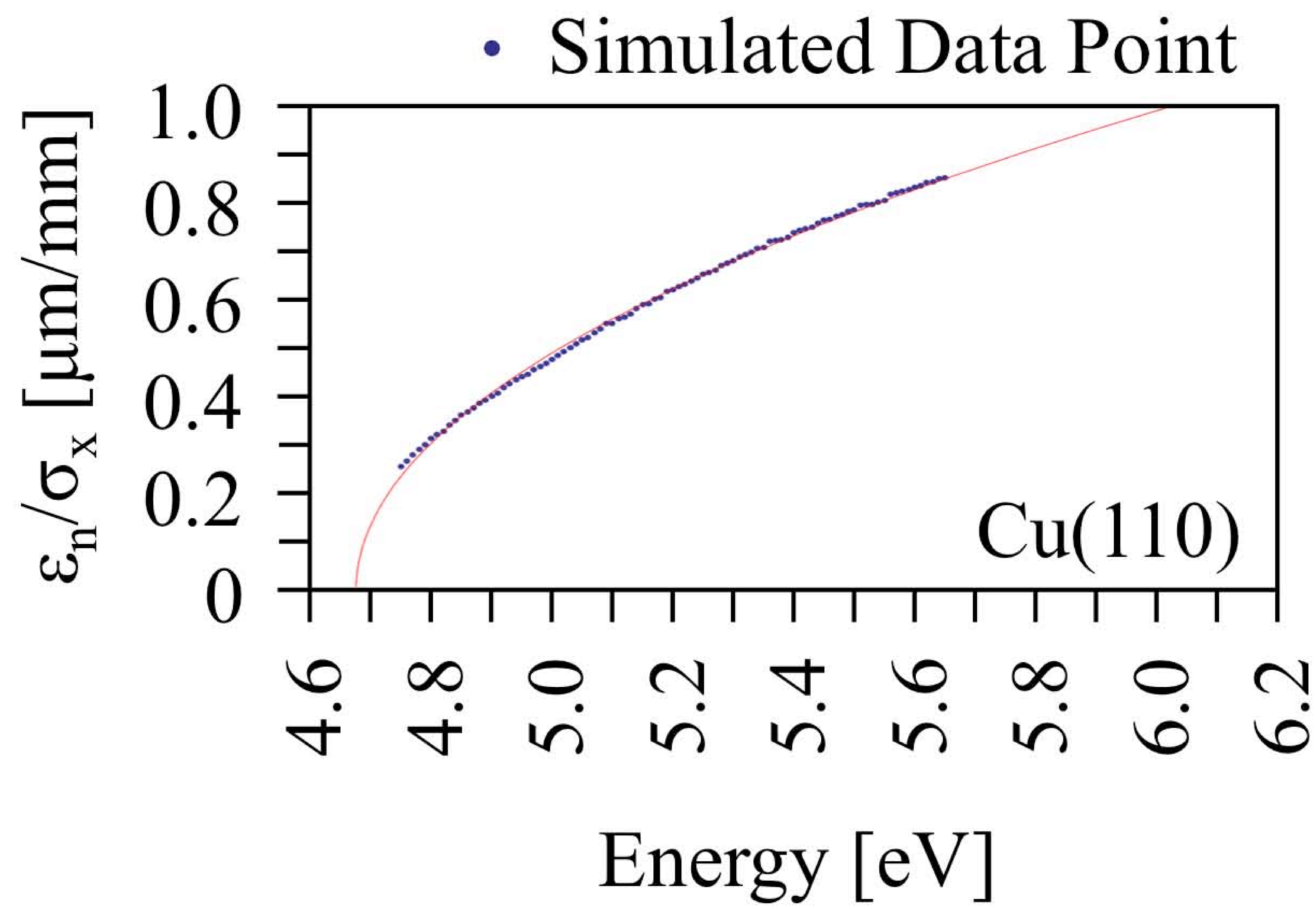

	φ, exp [eV]	φ, sim [eV]	m^* [m_e]
(100)	4.73 ± 0.10	4.78	0.98
(110)	4.56 ± 0.10	4.64	0.88
(111)	4.90 ± 0.02	5.01	…

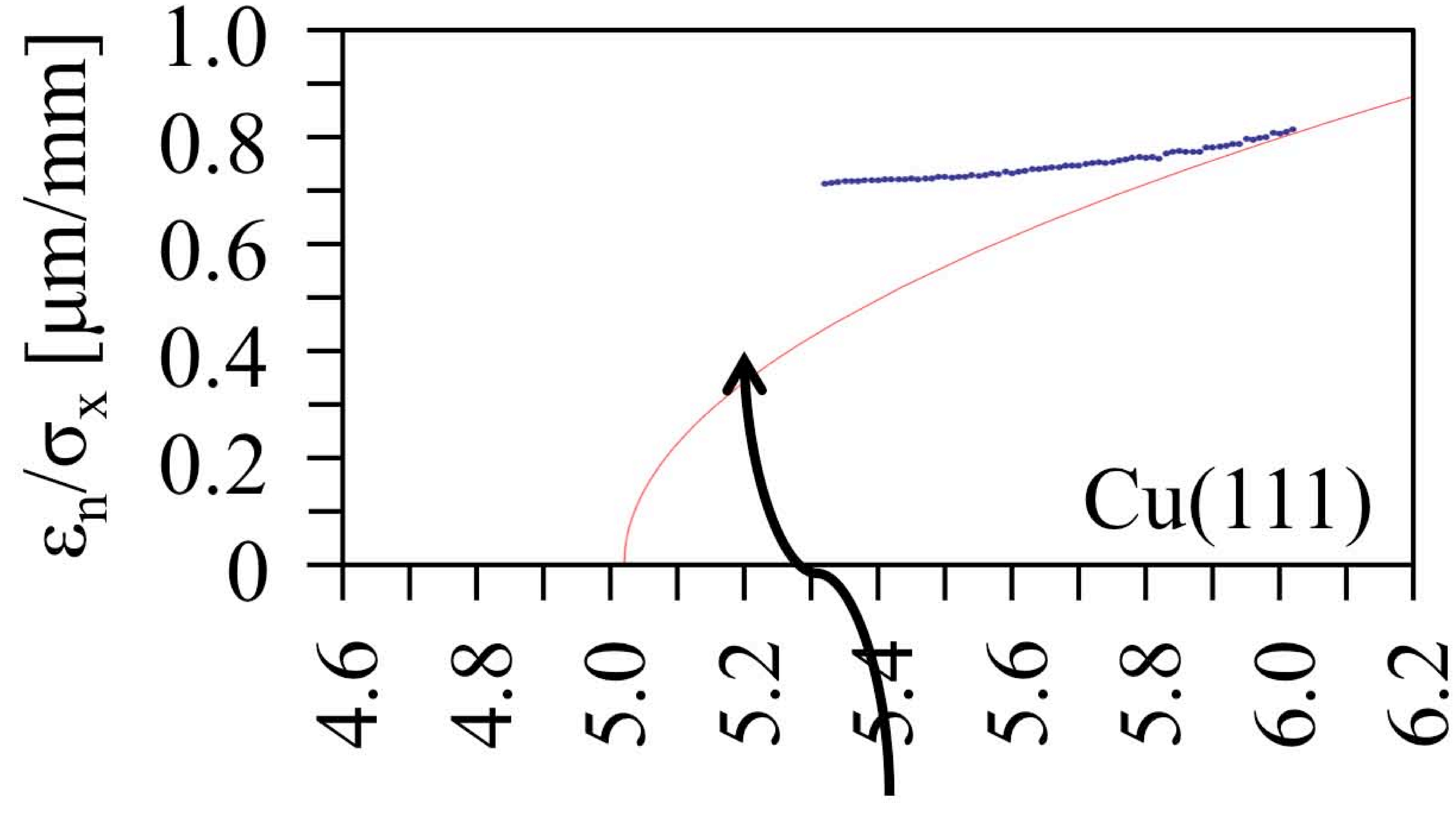

no emission!
(neck in the Fermi surface)

1.) T. Vecchione et al., Proc. of the 2015 International FEL Conf., Daejeon, Korea, WEP002.
2.) G. N. Derry, M. E. Kern and E. H. Worth, *JVSTA* **33**(6), 060801 (2015).

Simulated functional dependence of emittance and quantum efficiency on wavelength for copper (110) photocathodes

φ = 4.64 eV, gradient =120 MV/m, 30° phase (0.294 eV Schottky Effect)

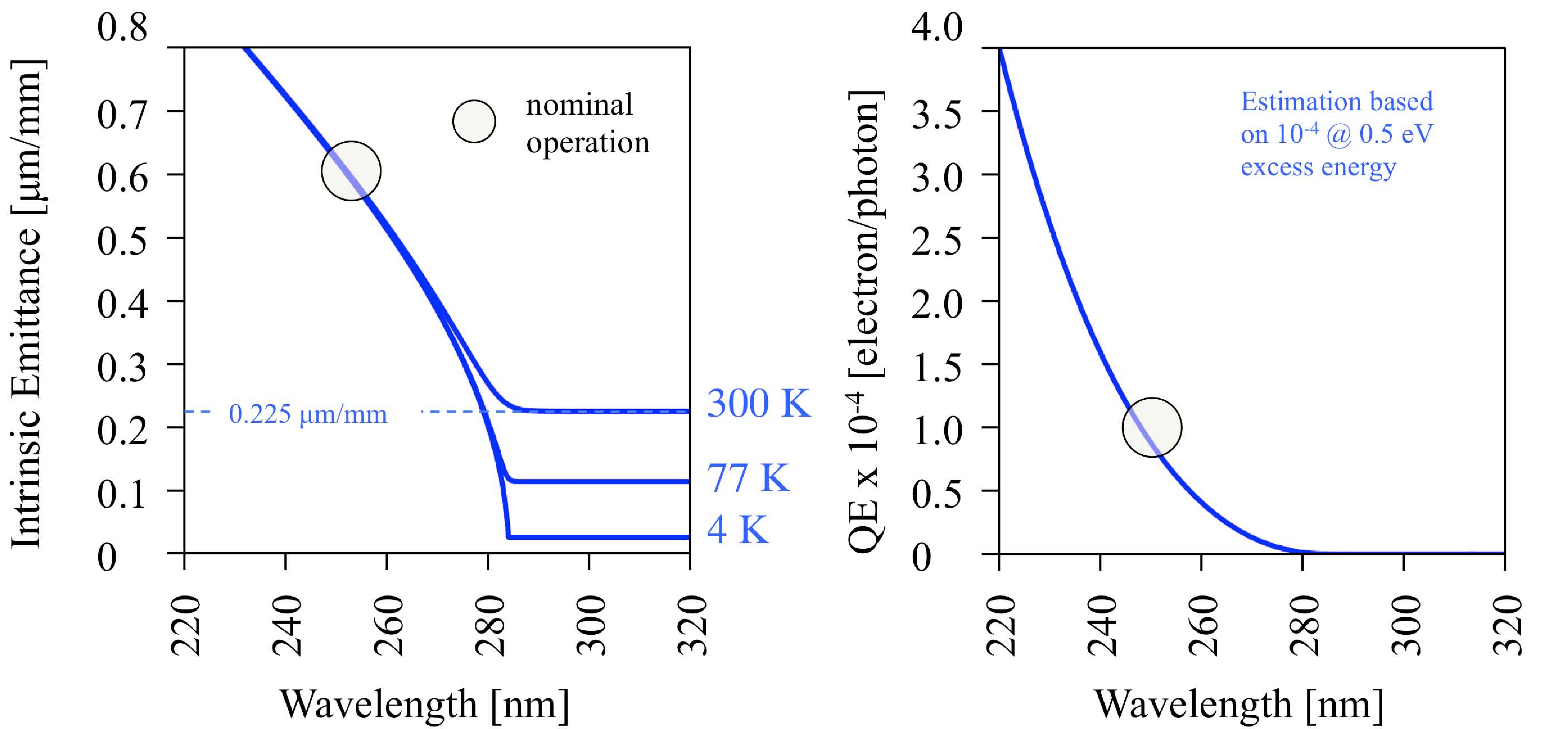

(110) surface has lowest work function, should dominate polycrystalline photocathodes

Predicted QE at 253 nm is ~1x10^{-4}, intrinsic emittance is 0.6 μm/mm

In reasonable agreement with values measured at the LCLS-I

"Known" Result: Change Wavelength to Reduce Emittance

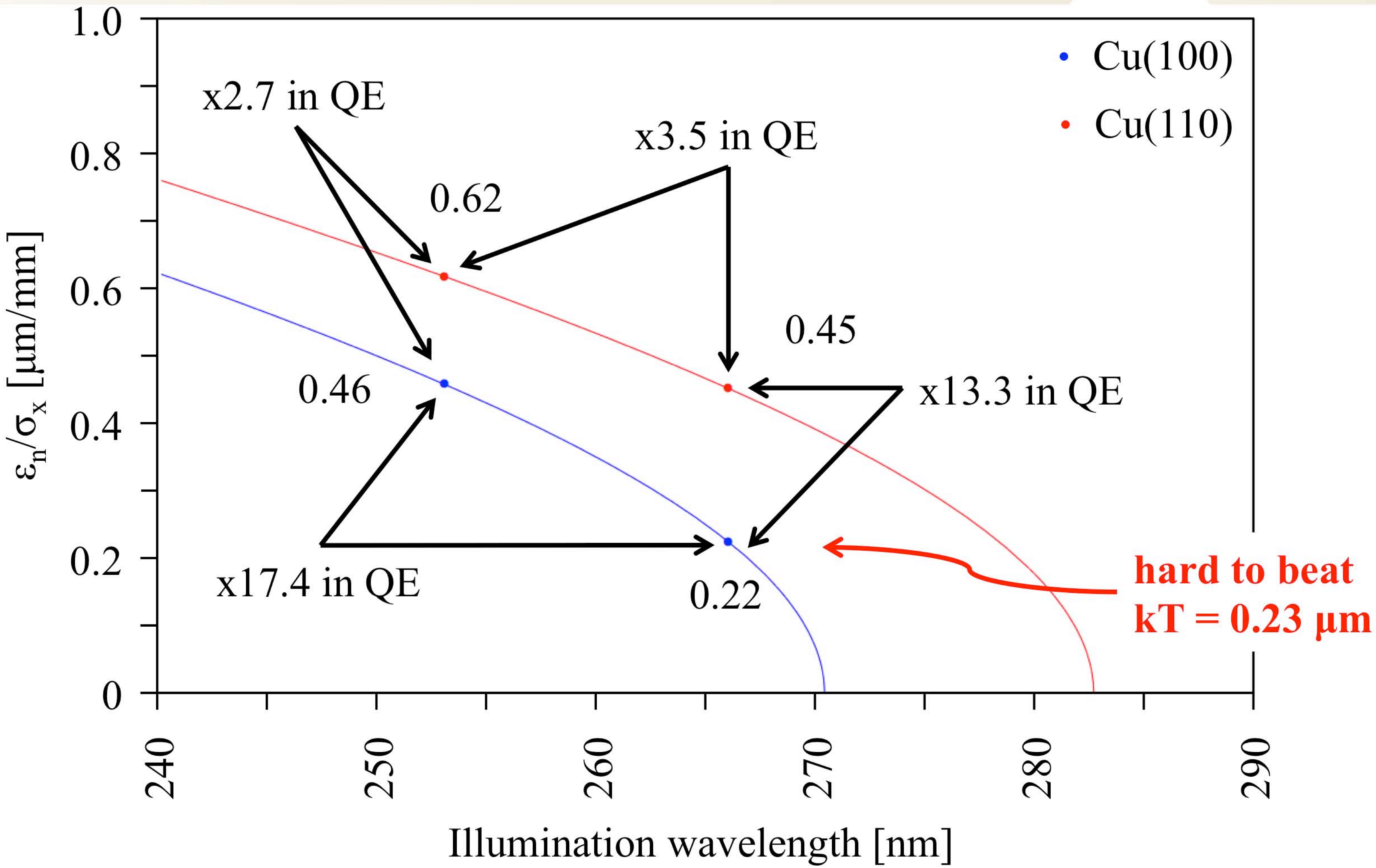

Changing laser from 253 to 266 nm → reduce intrinsic emittance by 25%
Requires enough laser power to make up for the lost charge (70% QE drop)

Future Plans

1.) **Include** effects of: finite temperatures, surface oxide layers & surface states

Use dispersion to generate low emittance
- Energy of transition (ħω) limits final allowed transverse momentum
- Anisotropic emission confined in both energy and momentum

surface state dispersion

no emission

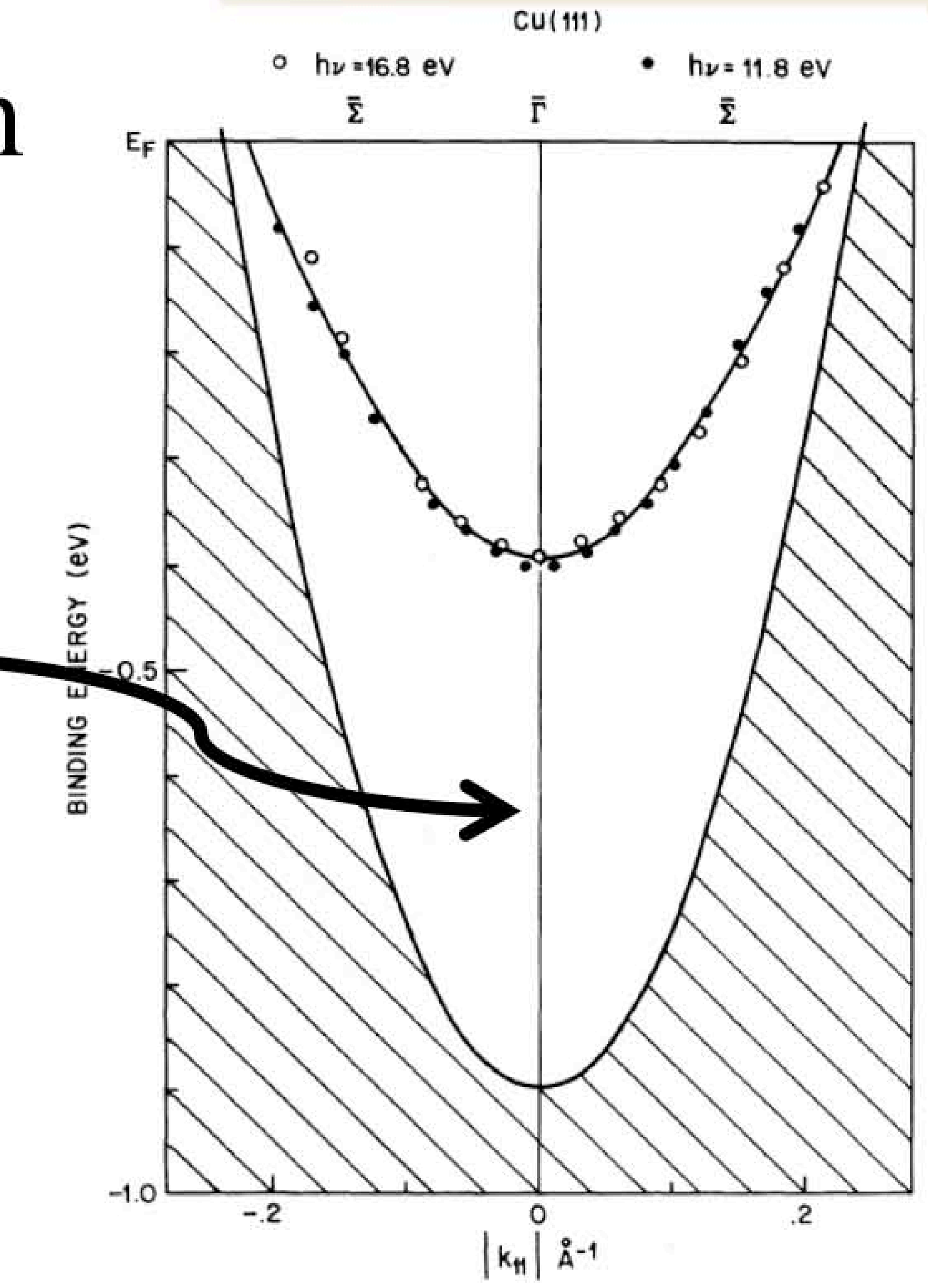

Reproduced from S. D. Kevan, *Phys. Rev. Lett.* **50** 7, 526 (1983).

2.) **Characterize single crystal surfaces** that support surface states, searching for small effective masses

(111) surfaces of FCC noble metals
(100) surfaces of BCC group VB & VIB
HCP metals w/ high lattice asymmetry

Li	Be									
Na	Mg									
K	Ca	Sc	Ti	V	Cr	Mn	Fe	Co	Ni	Cu
Rb	Sr	Y	Zr	Nb	Mo	Tc	Ru	Rh	Pd	Ag
Cs	Ba		Hf	Ta	W	Re	Os	Ir	Pt	Au

bcc
fcc

3.) **Transition to studying semiconductor photocathodes** for the LCLS-II, searching for small effective masses at their band gaps

Summary

LCLS-II injector team has begun fabricating components and is preparing for installation and commissioning next year.

There is lots of exciting work to be involved in over the next several years, including both injector and photocathode R&D

Thank you all for your attention!

Work supported by US DOE contract DE-AC02-76SF00515.